

Localization Efficiency in Massive MIMO Systems

Masoud Arash, *Student member, IEEE*, Hamed Mirghasemi, *Member, IEEE*, Ivan Stupia, *Member, IEEE*, Luc Vandendorpe, *Fellow, IEEE*

Abstract—In the next generation of wireless systems, Massive MIMO offers high angular resolution for localization. By virtue of large number of antennas, users' angle of arrival can be estimated with high accuracy. As Massive MIMO antenna array can be very large, the channels seen by different antennas might differ from each other, however, this does not rule out the possibility of the Angle of Arrival (AoA) estimation. We show that Cramer-Rao Lower Bound (CRLB) in multi-user independent, identically distributed (i.i.d) channels does exist and regardless of channel distribution, it converges toward a closed-form expression. Then, we redefine a localization efficiency function for a multi-user scenario and numerically optimize it with respect to the number of antennas. We prove when only a subset of the available antennas is used, CRLB can be minimized with respect to which set of antennas is used. An antenna selection strategy that minimizes CRLB is proposed. As a benchmark, we apply the proposed antenna selection scheme to the Multiple Signal Classification (MUSIC) algorithm and study its efficiency. Numerical results validate the accuracy of our analysis and show significant improvement in efficiency when the proposed antenna selection strategy is employed.

Index Terms—Massive MIMO, CRLB, Angle of Arrival, Localization Efficiency, Antenna Selection.

I. INTRODUCTION

Massive MIMO systems are one of the prime candidates for the next generation of wireless systems [1]. These systems employ a large number of antennas which provides numerous opportunities for performance improvement of a wireless system, like increased capacity, spatial diversity and lower latency [1]. Interestingly, these systems offer high accuracy for different kinds of localization, especially AoA and orientation of User Terminals (UTs) [2], [3]. In addition to these benefits, the use of massive antenna arrays would enable a more efficient use of the time and frequency resources by enabling the simultaneous localization of more UTs.

Various types of localization with different goals are introduced in the literature. Anchor Based schemes in which UTs' locations are estimated with respect to an anchor are one of the most popular methods [4]. In such approaches, methods like Received Signal Strength (RSS), Difference Time of Arrival and AoA estimation are used to map UTs' locations. Performance of these methods are usually evaluated by the *CRLB* which gives a lower bound on the estimation error for any unbiased estimator [5].

Several works studied *CRLB* in Massive MIMO settings. For a planar antenna array, [6] approximated it for a fading

free channel. In [5] authors derived *CRLB* as a function of instantaneous parameters for AoA, angle of departure, delay, and orientation estimation of UTs for different scenarios when there is a dominant path either in Line of Sight (LoS) or Non-LoS. In [7] *CRLB* for AoA and channel gain is obtained in a Massive MIMO system with planar array for a single UT. Authors in [8] approximated *CRLB* for a single UT case of a planar array in mmwave case when multi-path effects are considered.

All works in [5], [7], [8], considered an identical channel coefficient from each UT to all the antennas at the BS. This means all antennas are fully correlated and antenna array has zero spatial diversity. The main hypothesis behind this common assumption is that all the UTs experience channels in which one or few dominant paths convey most of the received signal power to the BS. As a matter of fact, previous studies on localization in massive MIMO systems offer valuable insights about the information that can be extracted from the dominant components of the channel (if there is any), with the obvious consequence that if those components are shadowed the *CRLB* of systems may grow indefinitely. It is worth remarking that this assumption might be in contradiction to the original idea of developing massive MIMO technologies as an efficient solution to provide seamless and reliable links between UTs and BS even in the absence of LoS or clear dominant paths. This consideration is corroborated by many studies of Massive MIMO systems, such as [9], assuming that UTs have independent channel coefficients for different antennas.

Besides, the same infrastructure might be used for both localization and data transmission. In this case, to avoid one spatial diversity, which results from fully correlated channels, antennas are placed in a way to gain independence. For instance, in mmwave scenarios, a separation of few centimeters can do this. Moreover, different channel coefficients can stem from lack of LoS for some antennas, while others have it. This can happen in cylindrical arrays or a linear array that is long enough, especially in dense environments like cities. Therefore, there is a clear discrepancy between studies for data transmission and localization in massive MIMO systems. The question that arises here is how *CRLB* changes when different antennas have different channel coefficients? Or in other words, can we exploit the presence of massive antenna arrays to extract the AoA information even when the dominant components of the channel are shadowed or absent?

In this perspective, [10] tackled the problem of i.i.d channel coefficients for AoA estimation for the first time. However, due to mathematical complications of *CRLB* analysis, [10] only addresses the probability of AoA detection for a single UT. The first objective of this work is then to fill this gap by

The authors are with the Institute of Information and Communication Technologies, Electronics and Applied Mathematics (ICTEAM), Université catholique de Louvain, 1348 Louvain-la-Neuve, Belgium (E-mail: masoud.arash@uclouvain.be).

This work has been submitted to the IEEE for possible publication. Copyright may be transferred without notice, after which this version may no longer be accessible.

proposing a deterministic expression of the $CRLB$ for multiple UTs under the hypothesis of i.i.d. channel coefficients between antennas. In this regard, various ideas have been proposed to remove the effects of instantaneous nuisance parameters (e.g. fading channel coefficients) in $CRLB$. In [11], Miller and Chang introduced a performance metric obtained by taking the expectation from the $CRLB$ with respect to (w.r.t.) the nuisance parameter, while in [12] the authors defined a Modified $CRLB$ ($MCRLB$) by taking an expectation from Fisher Information Matrix (FIM). The downside of those proposals is that the proposed metrics depend on the particular channel probability distribution. This problem is worsened in multi-user (MU) MIMO systems. To the best of our knowledge, this is the first work proposing a closed-form solution for the $CRLB$ in MU Massive MIMO systems relying only on the statistics of the channel coefficients.

To achieve this, we take advantage of Random Matrix Theory (RMT) to prove that the $CRLB$ of a MU Massive MIMO system almost surely converges to a deterministic function of the channel variance for all possible distributions of the channel coefficients, and we provide a closed-form expression for it. We also show that $CRLB$ for AoA estimation always converges to a finite value, meaning that AoA information can still be extracted also in the absence of any dominant path. This result is of particular importance to give a theoretical foundation to those techniques, such as the ones proposed in [2], [13], [14], aiming at exploiting multi-path signals to extract or refine AoA estimation when LoS signal may be extremely weak or absent, e.g. in vehicular localization.

Though Massive MIMO technology may guarantee seamless and reliable localization for multiple UTs with limited time and frequency resources, those benefits may be jeopardized by the increased energy consumption of those systems. The energy efficiency concern in Massive MIMO systems has drawn many research interests during last years [9], [15]. In [9], authors discussed how a realistic model for such systems should consider energy consumption of different parts, including hardware and signal processing units. Some of these parts that include computational and hardware energies, scale with the number of antennas. Accordingly, several works have studied how performance criteria change by considering such a realistic model [16], [17]. Efficiency in localization is only studied in few works and mainly at the network level. In [18] authors discussed the product of error and power consumption of a wireless sensor network as an efficiency parameter. [19] used the inverse of this product to give a physical sense to this criterion in same settings, obtaining $CRLB$ through simulations. Yet, the concept of efficiency in localization demands more attention as it can reflect important trade-offs.

For this reason, in the second part of this work, we redefine a Localization Efficiency (LE) function so it can be used for extensive studies in MU scenarios. First, LE is formulated with fundamental performance metrics, using obtained $CRLB$ for a typical system, number of UTs and total energy consumption. Contrary to previous studies, we use a realistic energy consumption model. Next, antenna selection is studied and it is shown that different sets of antennas change

$CRLB$'s (and consequently LE 's) behavior and formulation. Also, we show that optimal number of antennas is changed for various antenna selection strategies. Finally, to analyze LE and antenna selection in simpler system models, the MUSIC algorithm is studied. The contributions of this paper are summarized as follows:

- $CRLB$ for AoA estimation of a MU Massive MIMO system is derived in a deterministic form under i.i.d channel model with unknown distribution, using RMT methods.
- Efficiency function for localization is redefined as a function of system parameters for the evaluation of localization methods and it is used to study the trade-off between performance and energy consumption.
- Antenna selection for localization is introduced and a strategy of selection that minimizes $CRLB$ is presented. LE is reformulated in this case and the optimal number of antennas is obtained for this selection method.
- LE of MUSIC algorithm based on its exact required computations is derived. Also, different antenna selection methods are studied for this algorithm.

The remainder of this paper is organized as follows. In Section II we introduce our system model. $CRLB$ is calculated for different channel models of BS's antennas in Section III. LE is formulated in Section IV. All of these are then used to study the idea of antenna selection in Section V. LE of the MUSIC algorithm is dealt with in detail in Section VI. In Section VII, numerical results are used to validate the theoretical analysis and make comparisons of LE under various scenarios. Finally, the major conclusions are drawn in Section VIII.

Notation: Boldface lower case is used for vectors, \mathbf{x} , and upper case for matrices, \mathbf{X} . \mathbf{X}^* , \mathbf{X}^T , \mathbf{X}^H and $\mathbf{X}_{k,k}$ denote conjugate, transpose, conjugate transpose and (k, k) th entry of \mathbf{X} , respectively. $\mathbb{E}\{\cdot\}$ denotes expectation, $Card(\cdot)$ is cardinality of a set, $j = \sqrt{-1}$, $|\cdot|$ stands for absolute value of a given scalar variable, tr is trace operator, \odot is Hadamard product operator and $\xrightarrow{a.s.}$ means Almost Sure convergence. Also, \mathbf{I}_K is $K \times K$ identity and zero matrix. When $\mathbf{y} = [y_1 \ y_2 \ \dots \ y_p]^T$ and $\mathbf{x} = [x_1 \ x_2 \ \dots \ x_q]^T$, we define

$$\left(\frac{\partial \mathbf{y}}{\partial \mathbf{x}}\right)_{p,q} = \frac{\partial y_p}{\partial x_q}. \quad (1)$$

II. SYSTEM MODEL

We consider the uplink of a single-cell Massive MIMO system with a BS at the center of the cell, equipped with M antennas, equally separated by distance d (Fig. 1). There are K single antenna UTs distributed all over the cell. In this system, BS estimates UTs' AoA and channel coefficients using the pilot signals transmitted by UTs with wave length λ . The received signal at the BS side is

$$\mathbf{y} = \mathbf{G}\mathbf{s} + \mathbf{n}, \quad (2)$$

in which \mathbf{G} is $M \times K$ channel matrix between M BS antennas and K UTs, $\mathbf{s} \in \mathbb{C}^{K \times 1}$ is the vector of transmitted pilots and $\mathbf{n} \sim \mathcal{CN}(0, \sigma_n^2 \mathbf{I}_M)$ is additive noise. Without loss of generality, in addition to M antennas, we consider a reference

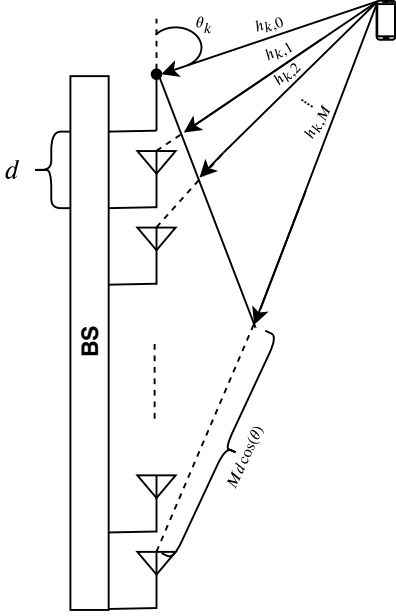


Figure 1: Antenna array configuration for i.i.d channels.

point at the BS side, on the top of the first antenna with the distance exactly equal to antenna separation distance and measure the AoA w.r.t. this point. Matrix \mathbf{G} is composed as

$$\mathbf{G} = (\mathbf{A}_{Rx} \odot \mathbf{H}) \mathbf{B}^{\frac{1}{2}}, \quad (3)$$

where

$$\mathbf{A}_{Rx} = [\mathbf{a}_{Rx,1}(\theta_1) \quad \mathbf{a}_{Rx,2}(\theta_2) \quad \dots \quad \mathbf{a}_{Rx,F}(\theta_K)] \quad (4)$$

contains $M \times 1$ steering vectors of BS antenna array response for K UTs in which

$$\mathbf{a}_{Rx,k}(\theta_k) = \frac{1}{\sqrt{M}} [e^{-j\beta \cos(\theta_k)} \quad \dots \quad e^{-jM\beta \cos(\theta_k)}]^T, \quad (5)$$

θ_k is k th UT's AoA for $k \in \{1, 2, \dots, K\}$ and $\beta = \frac{2\pi d}{\lambda}$. \mathbf{H} is an $M \times K$ matrix whose (m, k) th element, $h_{m,k}$, is fast fading coefficient between k th UT and m th BS antennas

$$h_{m,k} = h_{m,k}^r + j h_{m,k}^i, \quad (6)$$

and

$$\begin{aligned} \mathbb{E}\{h_{m,k}^r\} &= \mathbb{E}\{h_{m,k}^i\} = 0, \\ \mathbb{E}\{|h_{m,k}^r|^2\} &= \mathbb{E}\{|h_{m,k}^i|^2\} = \sigma_h^2, \end{aligned} \quad (7)$$

for $m \in \{1, 2, \dots, M\}$ and $k \in \{1, 2, \dots, K\}$. \mathbf{B} is an $K \times K$ diagonal matrix whose k th diagonal element contains large scale fading coefficients of corresponding UT

$$\mathbf{B}_{k,k} = l(r_k), \quad (8)$$

where $l(\cdot)$ is the path loss function, r_k is k th UT's distance from BS. Also, for simplicity, we define received signal to noise ratio at the BS side as

$$\rho_k \triangleq \frac{|s_k|^2}{\sigma_n^2 l(r_k)}. \quad (9)$$

III. CRLB

In this section, we derive *CRLB* of AoA and channel coefficients. For clarity, first we set our desired parameter to be $\cos(\theta)$ instead of θ , then same methods are applied to obtain corresponding results for θ . Desired parameters' vector will be

$$\boldsymbol{\eta} = \underbrace{[\cos(\theta_1) \quad \dots \quad \cos(\theta_K)]}_{\boldsymbol{\eta}_\theta} \underbrace{[\mathbf{h}_1^T \quad \dots \quad \mathbf{h}_K^T]}_{\boldsymbol{\eta}_h}^T, \quad (10)$$

where $\mathbf{h}_k = [h_{1,k} \quad \dots \quad h_{M,k}]^T$. Defining $\hat{\boldsymbol{\eta}}$ as the unbiased estimator of $\boldsymbol{\eta}$, the Mean Square Error (MSE) of the estimator is lower bounded as [5]

$$\mathbb{E}_{\mathbf{y}|\boldsymbol{\eta}}\{(\boldsymbol{\eta} - \hat{\boldsymbol{\eta}})(\boldsymbol{\eta} - \hat{\boldsymbol{\eta}})^T\} \geq \mathbf{CRLB} = \mathbf{J}^{-1}, \quad (11)$$

where \mathbf{J} is FIM and is defined as [5]

$$\mathbf{J} = \mathbb{E}_{\mathbf{y}|\boldsymbol{\eta}} \left[-\frac{\partial^2 \ln f(\mathbf{y}|\boldsymbol{\eta})}{\partial \boldsymbol{\eta} \partial \boldsymbol{\eta}^T} \right], \quad (12)$$

where $f(\mathbf{y}|\boldsymbol{\eta})$ is the likelihood function of the received signal. \mathbf{J} can be written in block matrix form as [7]

$$\mathbf{J} = \begin{bmatrix} \mathbf{J}_{\theta,\theta} & \mathbf{J}_{\theta,h} \\ \mathbf{J}_{h,\theta} & \mathbf{J}_{h,h} \end{bmatrix}, \quad (13)$$

where

$$\mathbf{J}_{a,b} = \frac{2}{\sigma_n^2} \mathcal{R}e \left[\left(\frac{\partial \mathbf{w}}{\partial \boldsymbol{\eta}_a} \right)^H \frac{\partial \mathbf{w}}{\partial \boldsymbol{\eta}_b} \right], \quad (14)$$

and $\mathbf{w} \triangleq \mathbf{G}\mathbf{s}$. Based on [7], in Massive MIMO settings, $\mathbf{J}_{\theta,h}$ and $\mathbf{J}_{h,\theta}$ can be approximated as zero matrices. In this case, by virtue of block matrix inversion lemma, we have

$$\mathbf{CRLB}_{\cos(\theta)} = \mathbf{J}_{\theta,\theta}^{-1} = \frac{\sigma_n^2}{2} \mathcal{R}e \left[\left(\frac{\partial \mathbf{w}}{\partial \boldsymbol{\eta}_\theta} \right)^H \frac{\partial \mathbf{w}}{\partial \boldsymbol{\eta}_\theta} \right]^{-1}, \quad (15)$$

and \mathbf{w} is

$$\mathbf{w} = \frac{1}{\sqrt{M}} \begin{bmatrix} \sum_{i=1}^K h_{1,i} s_i l(r_i) e^{-j\beta \cos(\theta_i)} \\ \sum_{i=1}^K h_{2,i} s_i l(r_i) e^{-j2\beta \cos(\theta_i)} \\ \vdots \\ \sum_{i=1}^K h_{M,i} s_i l(r_i) e^{-jM\beta \cos(\theta_i)} \end{bmatrix}. \quad (16)$$

Then,

$$\left(\frac{\partial \mathbf{w}}{\partial \boldsymbol{\eta}_\theta} \right)_{m,k} = \mathbf{X}_{m,k} = \frac{-jm\beta h_{m,k} s_k l(r_k) e^{-jm\beta \cos(\theta_k)}}{\sqrt{M}}. \quad (17)$$

for $m \in \{1, 2, \dots, M\}$ and $k \in \{1, 2, \dots, K\}$. So, using Eq. 11, *CRLB* will be

$$\mathbf{CRLB}_{\cos(\theta)} = \mathbf{J}^{-1} = \frac{\sigma_n^2}{2} (\mathcal{R}e(\mathbf{X}^H \mathbf{X}))^{-1}. \quad (18)$$

By virtue of the independence of antennas, using following lemmas from RMT, we prove that for any distribution of \mathbf{H} , $\mathbf{CRLB}_{\cos(\theta)}$ almost surely converges toward a closed-form expression that is a function of system parameters, such as number of antennas and variance of channel coefficients.

Lemma 1. Let $\boldsymbol{\Sigma} \in \mathbb{C}^{N \times N}$, be a matrix with uniformly bounded spectral norm. Let $\mathbf{x} \in \mathbb{C}^N$, be a random vector with i.i.d. entries of zero mean, variance $\frac{1}{N}$ and eighth order moment of order $O(\frac{1}{N^4})$, independent of $\boldsymbol{\Sigma}$. Then

$$\mathbf{x}^H \boldsymbol{\Sigma} \mathbf{x} - \frac{1}{N} \text{tr}(\boldsymbol{\Sigma}) \xrightarrow{a.s.} 0, \quad (19)$$

as $N \rightarrow \infty$.

Proof. See [20]. \square

Lemma 2. For $\Sigma \in \mathbb{C}^{N \times N}$, be a matrix with uniformly bounded spectral norm, \mathbf{x} and \mathbf{y} two vectors of i.i.d. variables such that $\mathbf{x} \in \mathbb{C}^N$ and $\mathbf{y} \in \mathbb{C}^N$ have zero mean, variance $\frac{1}{N}$ and fourth order moment of order $O(\frac{1}{N^2})$, we have

$$\mathbf{x}^H \Sigma \mathbf{y} \xrightarrow{a.s.} 0. \quad (20)$$

Proof. See [20]. \square

Theorem 1. In a Massive MIMO system with large number of antennas, $CRLB_{\cos(\theta)}$ converges toward a deterministic form as

$$CRLB_{\cos(\theta)} \xrightarrow{a.s.} \frac{3}{2\beta^2 \sigma_h^2 (M+1)(2M+1)} \mathbf{C}, \quad (21)$$

where \mathbf{C} is an $K \times K$ diagonal matrix with

$$C_{k,k} = \rho_k^{-1}, \quad k \in \{1, \dots, K\}. \quad (22)$$

Proof. See Appendix A. \square

When the exact AoA, θ , is the desired estimation parameter, we have

$$\boldsymbol{\eta}_\theta = [\theta_1 \quad \theta_2 \quad \dots \quad \theta_K]^T. \quad (23)$$

In this case, the following theorem gives the deterministic form of $CRLB_\theta$.

Theorem 2. For large number of antennas, we have

$$CRLB_\theta \xrightarrow{a.s.} \frac{3}{2\beta^2 \sigma_h^2 (M+1)(2M+1)} \mathbf{S}, \quad (24)$$

in which \mathbf{S} is an $K \times K$ diagonal matrix with

$$S_{k,k} = (\rho_k \sin^2(\theta_k))^{-1}, \quad k \in \{1, \dots, K\}. \quad (25)$$

Proof. See Appendix B. \square

It is seen from Eq. 21 and Eq. 24 that in a Massive MIMO system, regardless of channel distribution, instantaneous $CRLB$ tends toward a deterministic value. Although other definitions like Miller-Chang version [11] or $MCRLB$ [12] obtain a deterministic form for $CRLB$, they use expectation that requires the knowledge of channel coefficients' distribution. By contrast, our obtained expressions require only the knowledge of the variance of channel coefficients and is applicable even when the distribution of channel coefficients is unknown.

$CRLB$ in a Massive MU-MIMO system is inversely related to the second-order of number of antennas that is in accordance with previous analysis of these systems in [7], [8]. However, when there is not a dominant path, Eq. 21 and Eq. 24 show that $CRLB$ almost surely becomes a function of the variance of channel coefficients, instead of their instantaneous realizations. In other word, as the number of antennas grows, $CRLB$ becomes a function of general statistics of the channel, instead of individual realizations. This is because as the number of antennas grows, it is almost surely improbable that all antennas be in poor condition, simultaneously. So, even if few antennas have a low fading coefficient, not all of the information in

the system is lost and AoA can still be extracted. Same phenomenon also happens for channel capacity in these systems [9].

Recently several works have attempted to use path-loss signals, with different channel coefficients, to improve their estimation accuracy, such as [2], [13]. In [14] authors extracted location information (including AoA) without a dominant path using neural networks. These works show that in Massive MIMO systems AoA information can be extracted, even when LoS signal is obscured, using several path-loss signals with same order of power. Our theoretical results are in accordance with these works and confirm that $CRLB$ in such scenarios is finite and estimating AoA is possible.

IV. LOCALIZATION EFFICIENCY

In this section, we formulate LE function, which will aggregate benefits and costs of a localization method. To make a general criterion for different kinds of localization, we use parameters that are included in most of the localization methods. These parameters are, in the one hand, the number of UTs that are being localized simultaneously and localization accuracy of the method as benefit parameters and on the other hand, total energy consumption of a system in localization phase as cost parameter.

A. Accuracy Function

Accuracy is one of the major evaluation parameters in localization [21], [22]. Different works have studied the accuracy function of localization methods and optimized it w.r.t. various parameters. Generally, accuracy is defined as the trace of the inverse of equivalent FIM [21], [23], or as inverse of second root the trace of the $CRLB$ matrix [22]. As we have achieved a deterministic expression for $CRLB$, we use inverse of second root of its trace for accuracy function

$$Accuracy = \frac{1}{\sqrt{\text{tr}(\mathbf{CRLB}_\theta)}}. \quad (26)$$

B. Energy Consumption

Nowadays, one of the key parameters of a wireless system is energy consumption [9]. Due to growing concerns about energy, designers have to carefully consider the energy consumption of their systems and include it in system characterization. Analyzing energy consumption of a system indicates at what cost a performance is obtained. As an example, energy efficiency of wireless systems has been widely used to describe performance trade-off between rate and energy consumption [9], [17].

In order to conduct a comprehensive investigation, it is of paramount importance to consider energy consumption of all parts of a wireless system. In addition to transmitted power, in a Massive MIMO system, energy consumption of system hardware should also be considered to obtain a realistic model [9]. For instance, energy consumption of antennas' RF-chains and processing units, that scale with number of antennas, is not negligible in Massive MIMO systems. In the following, we investigate different parts of total energy consumption function according to our system model.

$$LE = \frac{K\sqrt{2\beta^2\sigma_h^2(M+1)(2M+1)}}{\sqrt{3}\zeta\left(\frac{W}{L_{BS}}K^M + MP_{BS} + KW\sum_{i=1}^K\|s_i\|^2 + KP_{UT} + P_{fix}\right)\sqrt{\text{tr}(\mathbf{S})}}. \quad (32)$$

1) *Transmitted Energy*: In the uplink of a wireless system, UTs transmit pilots to become localized by the BS. Usually, this energy is very important as UTs have limited energy budget. This is one of the main reasons which prevents broad utilization of methods like GPS, in the next generation of wireless systems. Pilot signals are predefined with certain energy. This energy is linearly related to number of UTs. Therefore, transmitted energy will be

$$E_{tr} = \zeta W \text{tr}(\mathbf{s}\mathbf{s}^H) = W\zeta \sum_{i=1}^K |s_i|^2 \quad (J), \quad (27)$$

in which ζ and W are duration and bandwidth of transmitted pilots, respectively.

2) *Processing Energy*: We assume that the BS carries out all of the required processing. As far as LE is concerned, these processes include the detection of pilots and running localization algorithm. This energy is proportional to number of operations which in turn is a function of system parameters such as M and K . To evaluate the energy consumption of this part, one needs to calculate number of required operations of an algorithm and also the computational efficiency of BS processing hardware. Generally, Maximum-likelihood (ML) method that obtains $CRLB$ has the calculation complexity of K^M [24]. This is the worst case and there may be ways to reduce number of required calculations. Sub-optimum algorithms have M^3 order of complexity, at most, but they do not necessarily obtain $CRLB$. We study one of these algorithms in section VI. Computational efficiency, $L_{BS}(FLOP/J)$, is usually expressed as number of Floating Point Operations (FLOP) per Second per Watt that hardware consumes [9]. So, assuming same time as pilot transmission is used for processing, the processing energy consumption, E_p , for ML will be formulated as

$$E_p = \frac{K^M}{L_{BS}} W\zeta \quad (J). \quad (28)$$

3) *Hardware Energy Consumption*: Generally, hardware of a wireless system can be divided into two parts:

- Infrastructure part of a system that includes backhaul systems and network part, cooling system and so on, which use a constant energy and are necessary for system maintenance.
- RF-chains of BS and UTs' antennas that are proportional to number of BS antennas and number of UTs.

Therefore, hardware energy consumption, E_h will be

$$E_h = \zeta(MP_{BS} + KP_{UT} + P_{fix}) \quad (J), \quad (29)$$

where P_{BS} and P_{UT} are BS and UTs' RF-chain power consumption, respectively and P_{fix} accounts for all powers that are not related to M .

Therefore, total energy consumption will be

$$E_t = E_{tr} + E_p + E_h. \quad (30)$$

Finally we can formulate LE as

$$LE = \frac{K(\text{Accuracy})}{\text{EnergyConsumption}} = \frac{K}{(E_t)(\sqrt{\text{tr}(\mathbf{CRLB}_\theta)})}. \quad (31)$$

Replacing all equations by their formula, LE is written as Eq. 32, at the top of this page. In this equation, LE is a function of several system parameters, such as M , K and θ . Although designers usually cannot control some parameters such as UT's AoA or their number, they do have access to number of BS antennas. As LE reflects a trade-off between accuracy and energy consumption, this creates an opportunity that can be used to design a system that operates in optimal point of this trade-off. In Eq. 32, it can be seen that both nominator and denominator are increasing functions of number of antennas, which suggests an optimum point might exist for M that maximizes LE . Unfortunately, analytical optimization of Eq. 32 is very complicated. To maximize it w.r.t. M , numerical methods will be used in section VII. Our results confirm that there is an optimum point for Eq. 32 and LE is significantly higher using optimal number of antennas instead of all of them. This means depending on the number of UTs and other system parameters, it will be more energy efficient to use only a subset of available antennas at the BS.

When number of optimal antennas is smaller than total available antennas, there is an opportunity to further increase LE by selecting a set of antennas whose contribution is higher than others. In the next section, this subject is studied.

V. ANTENNA SELECTION

In this section, we analyze the effect of antenna selection in a Massive MIMO system for localization. When number of utilized antennas is smaller than total available antennas, e.g. due to LE optimization or fewer available RF-chains, there is an opportunity that if a specific set of antennas are deployed, LE can be improved even more. Energy consumption of the system in Eq. 30 is only a function of number of antennas, independently which antennas are being used. On the other hand, in addition to number of antennas, $CRLB$ is a function of the set of antennas that are being used. To show this, we recall Eq. 65 that states $CRLB$ is inversely proportional to $\text{tr}(\mathbf{\Sigma})$. Assuming optimal number of antennas (or available RF-chains) is F , to minimize $CRLB$, $\text{tr}(\mathbf{\Sigma})$ has to be maximized by choosing a subset of utilized antennas \mathcal{S} . So, we have

$$\begin{aligned} & \max_{\mathcal{S} \subset \{1, \dots, M\}} \sum_{x \in \mathcal{S}} x^2 \\ & \text{s.t. } \text{Card}(\mathcal{S}) = F. \end{aligned} \quad (33)$$

Optimal solution for this problem consists of the last F antennas

$$\mathcal{S}^* = \{(M - F + 1), \dots, M\}, \quad (34)$$

$$LE_S = \frac{K\sqrt{2\beta^2\sigma_h^2(6M(M-F+1) + (F-1)(2F-1))}}{\sqrt{3}\zeta\left(\frac{W}{L_{BS}}K^F + FP_{BS} + KW\sum_{i=1}^K\|s_i\|^2 + KP_{UT} + P_{fix}\right)\sqrt{\text{tr}(\mathbf{S})}}. \quad (40)$$

that results in the maximum value for the trace as

$$\sum_{x=M-F+1}^M x^2 = \frac{F(6M(M-F+1) + (F-1)(2F-1))}{6}. \quad (35)$$

and minimum $CRLB$ for \mathbf{S}^* as

$$CRLB_{\theta}^* \xrightarrow{a.s.} \frac{3}{2\beta^2\sigma_h^2(6M(M-F+1) + (F-1)(2F-1))} \mathbf{S}. \quad (36)$$

It should be noted that when we want to use F antennas, the normalization factor in Eq. 5 become $F^{-\frac{1}{2}}$ instead of $M^{-\frac{1}{2}}$. The interpretation of Eq. 34 is that if for any reason fewer antennas than available antennas should be used, optimal choice is to start selecting antennas from the furthest antenna w.r.t. the reference point and move toward it. We recall this set of antennas as the *furthest set*. With this approach, $CRLB$ will be dramatically reduced relative to the case when we choose antennas from the beginning of the array. For comparison, we write $CRLB_{\theta}$ when F first antennas (*first set*) are used

$$CRLB_{\theta} \xrightarrow{a.s.} \frac{3}{2\beta^2\sigma_h^2(F+1)(2F+1)} \mathbf{S}. \quad (37)$$

It can be seen from Eq. 36 and Eq. 37 that while $CRLB$ for the first set is only a function of F , it is a function of both F and M for the furthest set. In other words, first set antenna selection approach does not fully appreciate the presence of a large antenna array. Furthermore, $CRLB$ for the first set is a *decreasing* function of F , however, $CRLB$ of the furthest set will be an *increasing* function of F . The reason for this phenomenon lies within the normalization factor in Eq. 5 that results in the normalization of $\text{tr}(\mathbf{\Sigma})$. When we start adding antennas from the end of array, we start from an antenna with the largest contribution to the trace, M^2 , and minimum normalization cost, which is 1. Then, a smaller value is added but as the summation is normalized by the cardinality of the set, it will decrease, because for $x \geq 1$

$$\frac{x^2}{1} > \frac{x^2 + (x-1)^2}{2}. \quad (38)$$

Therefore, the denominator of $CRLB$ decreases, and in turn, $CRLB$ increases. This process is reversed for the first set of antennas. In this case, we start from an antenna with the lowest contribution to the trace and add higher values as we use more antennas. So, the normalized summation is increasing, because for $x \geq 1$

$$\frac{x^2}{1} < \frac{x^2 + (x+1)^2}{2}. \quad (39)$$

So, depending on the method that we select operating antennas, both $CRLB$'s formula and behavior w.r.t. number of utilized and all available antennas is changed. In this regard, using a set of antennas that are furthest from the reference point, minimizes $CRLB$.

If F furthest antennas in the array are selected for localization, LE 's formula will be changed to Eq. 40, presented at the top of this page.

Theorem 3. *When operating antennas are selected from the furthest set, optimal number of them is*

$$F^* = K + 1. \quad (41)$$

Proof. Eq. 30 and Eq. 36 clearly show that both E_t and $CRLB$ are increasing functions of F . Therefore, maximum value of LE in Eq. 40 happens for the minimum possible value of F which is $K + 1$. \square

Remark 1. *It should be noted that here it is assumed that received power to all of the antennas is same and phase difference of the signal in all of antennas can be extracted. However, when the array becomes too large, attenuation w.r.t. reference point may become so strong that phase difference cannot be extracted anymore. So, these results are for cases when all of M antennas can extract phase difference.*

In case of fully correlated antennas, based on results presented in [8], [7] for a single UT case, it is seen that $CRLB$ is still proportional with the inverse of $\text{tr}(\mathbf{\Sigma})$, which means our results for antenna selection is applicable for this setting, too. Therefore, no matter what the channel model is, by using proposed antenna selection method, $CRLB$ can be minimized and LE can be further improved.

VI. MUSIC ALGORITHM

In order to study antenna selection effects on system performance when all of the antennas have same channel coefficient, we use it for one of the most known algorithms for AoA estimation, MUSIC, which is being used in several applications [25]. We study its LE and how antenna selection improves it. This helps to clarify that antenna selection is beneficial, no matter what the channel model is. After a brief description of its procedure, we calculate the exact amount of calculations that are required by this algorithm and formulate its LE . Then in section VII we compare LE when antennas are selected from the furthest and first set.

A. Procedure

Consider that we have a received signal as

$$\mathbf{y}_F = \mathbf{A}_F \mathbf{s} + \mathbf{n}_F, \quad (42)$$

subscript F shows number of rows, as F antennas are deployed. Sample covariance matrix of this signal can be obtained as [26]

$$\tilde{\mathbf{R}}_y = \frac{1}{N} \sum_{i=1}^N \mathbf{y}_{F_i} \mathbf{y}_{F_i}^H. \quad (43)$$

Table I: Simulation parameters

Parameter	Value	Parameter	Value
Bandwidth: W	50KHz	Operational efficiency: L_{BS}	30(GFLOP/Joule)
Pilot transmission time: ζ	0.5(ms)	BS's RF-chain Power consumption: P_{BS}	1W
Noise variance: σ_n^2	10^{-20} (W/Hz)	UT's RF-chain Power consumption: P_{UT}	0.3W
Channel coefficients: h^r, h^t	$\mathcal{N}(0, 0.5)$	Fixed power consumption in BS: P_{fix}	0.5W
Received pilot power: p	10^{-19} (W/Hz)	Antenna separation ratio to wavelength: $\frac{d}{\lambda}$	0.5

In the Eigenvalue Decomposition (EVD) of $\tilde{\mathbf{R}}_y$, there will be K eigenvectors corresponding to K UTs and $F - K$ eigenvectors corresponding to the noise. Each noise eigenvector is orthogonal to the columns of \mathbf{A} . So, by forming \mathbf{E}_n , composed of noise eigenvectors,

$$\mathbf{E}_n = [\mathbf{v}_{K+1} \quad \mathbf{v}_{K+2} \quad \dots \quad \mathbf{v}_F], \quad (44)$$

we can form a spatial spectrum function as [27]

$$P(\theta_i) = \frac{1}{\mathbf{g}(\theta_i)^H \mathbf{E}_n \mathbf{E}_n^H \mathbf{g}(\theta_i)}, \quad (45)$$

in which \mathbf{g} is a subset of $\mathbf{a}_{R_x, k}$ for the antenna subset that is being used, e.g., if the furthest set of antennas is used it will be

$$\mathbf{g}(\theta_i) = \frac{1}{\sqrt{F}} [e^{-j(M-F+1)\beta \cos(\theta_i)} \quad \dots \quad e^{-jM\beta \cos(\theta_i)}]^T, \\ \theta_i \in [0, \frac{\pi}{Q}, \dots, \frac{\pi-1}{Q}], \quad (46)$$

where Q is search cardinality. Peaks of $P(\theta)$ happens when $\mathbf{g}(\theta)$ corresponds to one of the actual steering vectors. These peaks are estimated as AoAs. Therefore, steps of MUSIC are

- i) Observe N snapshots and construct $\tilde{\mathbf{R}}_y$ in Eq. 43.
- ii) Calculate the EVD of $\tilde{\mathbf{R}}_y$ and extract \mathbf{E}_n in Eq. 44.
- iii) Construct $P(\theta)$ and extract its maximum points.

B. Energy Consumption of MUSIC

To accurately determine the required energy consumption of the MUSIC algorithm, we first analyze number of its required operations. With the help of [28], we evaluate number of required arithmetic operations to run MUSIC.

In the first step, the algorithm multiplies an $F \times 1$ vector by its conjugate transpose N times, sum them and then divides all of its elements by N . Every product of the vectors requires F^2 operations, every matrix sum requires F^2 operations and the final divide needs F^2 operations [28]. So, first step needs $(2N + 1)F^2$ operations.

Generally, EVD of an $F \times F$ matrix by QR decomposition-based algorithm needs at least F^3 operations [28]. So, the second step demands F^3 operations.

In the last step, ignoring the search part, we need to calculate Eq. 45, Q times. Product of $\mathbf{E}_n \mathbf{E}_n^H$ needs $F^2(2(F - K) - 1)$ operations and then, multiplying the resulted $F \times F$ matrix by two $F \times 1$ vectors from both sides, needs $(2F - 1)(F + 1)$ operations. Therefore, third step requires $Q[2F^2(F - K) + F^2 + F - 1]$ operations.

So, total number of arithmetic operations of MUSIC is

$$N_A = (2Q + 1)F^3 + (2N + Q(1 - 2K) + 1)F^2 + QF - Q. \quad (47)$$

Consequently, processing energy consumption of MUSIC will be

$$E_p = \frac{N_A}{L_{BS}} W \zeta. \quad (48)$$

Considering same transmitted power for all UTs, p , E_{tr} is

$$E_{tr} = NW \zeta \text{tr}(\mathbf{s} \mathbf{s}^H) = NKW \zeta p, \quad (49)$$

Hardware energy consumption will be same as Eq. 29. Therefore, total energy consumption of localization process using MUSIC algorithm is

$$E_t = E_t + E_{tr} + E_h \\ = W \zeta \underbrace{\left(\frac{2Q + 1}{L_{BS}}\right)}_{C_3} F^3 + W \zeta \underbrace{\left(\frac{2N + 1 + Q(1 - 2K)}{L_{BS}}\right)}_{C_2} F^2 \\ + \underbrace{W \zeta \left(P_{BS} + \frac{Q}{L_{BS}}\right)}_{C_1} F \\ + \underbrace{W \zeta \left(NKp - \frac{Q}{L_{BS}} + KP_{UT} + P_{fix}\right)}_{C_0} = \sum_{i=0}^3 C_i F^i. \quad (50)$$

MSE of the MUSIC algorithm is defined as

$$MSE = \frac{1}{N_{MC}} \sum_{i=1}^{N_{MC}} \sum_{k=1}^K (\theta_k - \hat{\theta}_k)^2, \quad (51)$$

where N_{MC} is number of Monte-Carlo simulations of MUSIC algorithm.

Finally, we formulate the LE as

$$LE_{MUSIC} = \frac{K}{(E_t)(\sqrt{MSE})}, \quad (52)$$

In the next section, the MUSIC algorithm's LE is optimized w.r.t. F and its behavior when these F antennas are selected from the first and furthest set.

VII. NUMERICAL RESULTS

In this section, we verify our analytical results that are obtained in previous sections. we study behavior of LE function for different scenarios, using Monte-Carlo simulations when analytical traceability is not possible. Also, optimization for LE is done through Monte-Carlo simulations. Parameters that we use are listed in Table I, unless otherwise stated.

Fig. 2 shows $\text{tr}(\mathbf{CRLB}_\theta)$ in which dashed lines are generated by Monte-Carlo simulations (indicated by MC) while solid lines are computed using approximated expression in Eq. 37 for $K = 5, 20, 40$. As \mathbf{CRLB}_θ grows indefinitely when $\theta \rightarrow 0, \pi$, an area of $\pi/10$ from each side is excluded

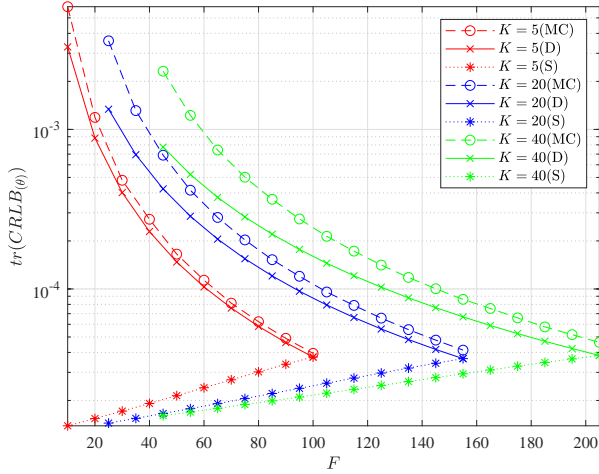


Figure 2: Deterministic and Monte-Carlo simulations of $CRLB_{\theta}$.

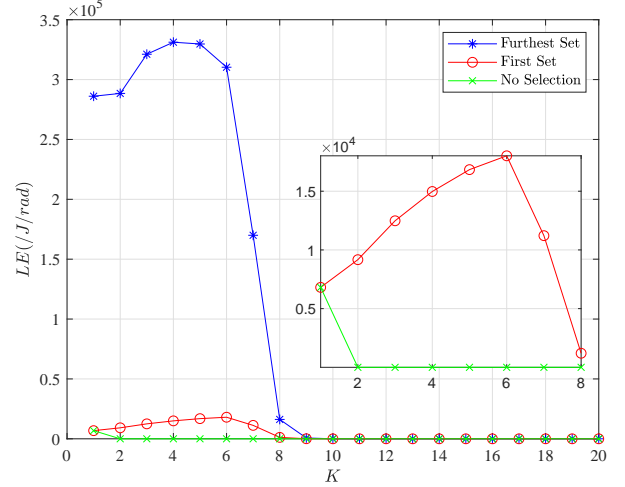


Figure 4: Optimal LE for each corresponding K in ML estimation.

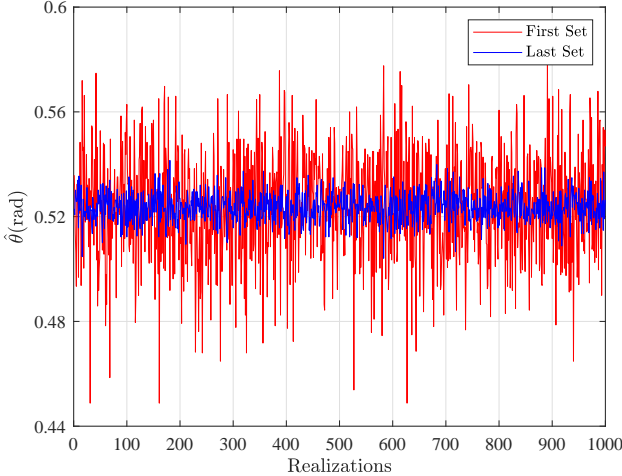


Figure 3: ML estimation for a single UT with $M = 16$.

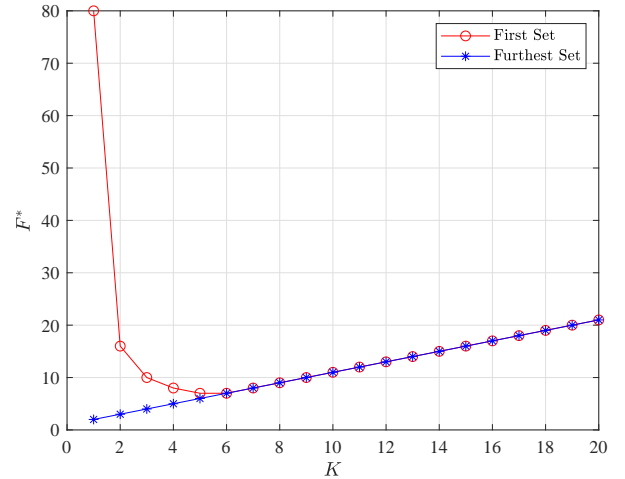


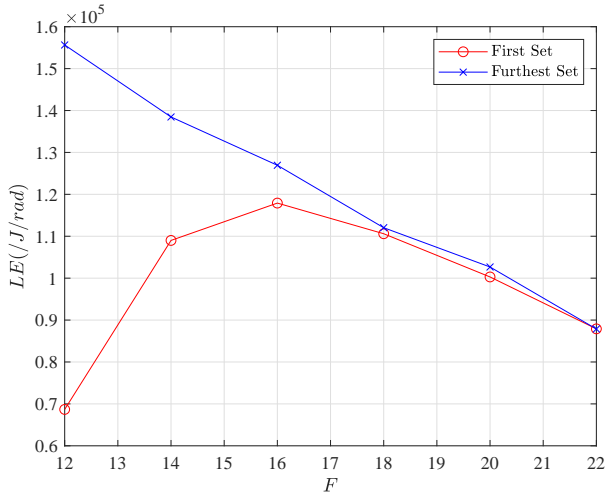
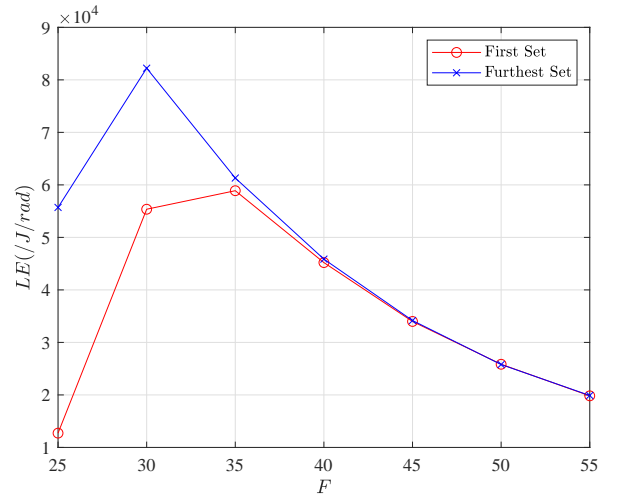
Figure 5: Optimal number of antennas for ML.

and UTs are equispaced in the remaining area. Interestingly, deterministic approximation (indicated by D) converges very fast, even when number of antennas is not so large. Also, Eq. 37 has same behavior as Monte-Carlo simulations. It should be noted that as the trace of $CRLB_{\theta}$ is plotted, the distance between analytical expression and Monte-Carlo simulations will increase for higher number of UTs, since it is sum of K almost sure convergence. This is why there is a seeming increment between analytical and Monte-Carlo curves in this figure. Furthermore, deterministic $CRLB_{\theta}$ in Eq.36, is plotted (indicated by S) when $M = 100, 155, 205$ for corresponding $K = 5, 20, 40$ curves. We see that there is a significant decrease in $CRLB_{\theta}$ when furthest set of antennas is used relative to the case when first group of them is used, more than two orders of magnitude in some cases. As number of utilized antennas grows, $CRLB_{\theta}$ for furthest set grows and becomes closer to the first set curve, until all available antennas are used, when they become same. The larger M ,

the lower the $CRLB_{\theta}$ will become, for the furthest set.

In Fig. 3 an ML estimator's output for a single UT is plotted to compare furthest and first antenna selection when number of antennas is not so large in Monte-Carlo simulations. In this figure, $M = 16$ and $F = 6$ and UT's AoA is $\theta = \frac{\pi}{6}$. It is seen that furthest set has dramatically lower variance in its estimation, proving that it outperforms antenna selection from the first set. Ratio of mean variance of furthest antenna set to first set is 0.066 in Monte-Carlo simulation and the ratio predicted by Eq. 36 and Eq. 37 is 0.061. This proves the accuracy of these deterministic equations.

In Fig. 4 LE for different numbers of UTs is plotted. In this figure, $M = 80$ and for the green curve (Eq. 32), in each K all of available antennas are used, i.e. no antenna selection. We see that due to high computational complexity, LE drops sharply as K increases. In other two curves (blue for Eq. 40 and red for replacing M with F in Eq. 32), for each K , LE is maximized w.r.t. F , with constraint $F \geq K$. We see that LE

Figure 6: LE of MUSIC for $K = 10$.Figure 7: LE of MUSIC for $K = 20$.

is significantly improved when optimal number of antennas is used instead of all available antennas. This confirms that using all of the antennas is not always efficient. Moreover, when optimal number of antennas are selected from the furthest set, LE increases even further, up to 220% in some points, which highlights the advantage of proposed antenna selection. As K increases, energy consumption increases exponentially and this causes LE of different scenarios decrease and become close to each other, however they are not exactly same until all of available antennas are used.

Fig. 5 shows corresponding optimal number of antennas for each K that maximize LE in Fig. 4. It is seen that due to exponential growth of energy consumption, F^* decreases very fast for the first set and reaches saturation point ($F^* = K + 1$) as K increases. Accordingly, this is the point after which LE starts to decrease in Fig. 4. Also, as predicted by Eq. 41, optimal number of antennas for the furthest set is always minimum possible number of antennas, $K + 1$. This illustrates that furthest antenna selection obtains higher LE using fewer number of antennas, which in turn reduces costs of construction and maintenance of the system.

LE of MUSIC algorithm is plotted by Monte-Carlo simulation of Eq. 52, for $K = 10$ and $M = 22$ in Fig. 6 and for $K = 20$ and $M = 55$ in Fig. 7. Same as Fig. 2, an exclusion area of $\pi/7$ is considered here. By selecting antennas from first set, LE has an optimum point in $F^* = 16$ and $F^* = 35$ in these settings, respectively. On the other hand, for furthest antenna selection, in $K = 10$, LE is always decreasing and so its optimum point is at minimum number of antennas, but in $K = 20$ LE of furthest set has an optimum point in $F = 30$. Nevertheless, its optimum point always happens before the optimum point of the first set, meaning that furthest antenna selection needs fewer antennas in this scenario, too. In addition, furthest antenna selection always has higher LE than first antenna selection proving that furthest antenna selection is always beneficial, no matter what the channel model is.

VIII. CONCLUSION

This paper analyzed $CRLB$ for AoA estimation when BS antennas have i.i.d channel coefficients. With the help of RMT, we proved that despite what channel coefficients' distribution is, $CRLB$ almost surely converges toward a closed-form expression in MU-Massive MIMO setting. This illustrates that AoA information can be extracted even when there is not a dominant path, providing a theoretical basis for recent studies that estimated location information in this scenario.

A refined version of the localization efficiency function is presented, which is a ratio of benefits to costs in localization and reflects the trade-off between performance and energy consumption. Contrary to previous studies, we used a realistic energy consumption model in this function and showed that there is an optimal number of antennas that maximizes the efficiency in localization phase. We presented an antenna selection method that minimizes $CRLB$ when number of utilized antennas is smaller than the total available antennas. Also, the behavior of both $CRLB$ and LE for this selection scheme is studied. It is shown that the behavior of both of them change when utilized antennas are selected based on proposed scheme and this affects the optimal number of antennas that maximizes LE .

Numerical results confirmed the $CRLB$'s convergence, even when number of antennas is not too large. They showed that the proposed antenna selection strategy dramatically reduces $CRLB$. This phenomenon has been validated by Monte-Carlo simulations, too. Furthermore, simulation results confirmed significant improvement of LE when our antenna selection approach is utilized. In fact, with the help of proposed antenna selection method, ML estimation gains a competitive advantage, in terms of efficiency, over a certain region. In the end, LE of the MUSIC algorithm is studied and simulated, indicating applicability of our antenna selection strategy even when all of the antennas have same channel coefficient.

IX. ACKNOWLEDGEMENT

This work is supported by F.R.S.-FNRS under the EOS research project MUSEWINET (EOS project 30452698).

REFERENCES

- [1] E. G. Larsson, O. Edfors, F. Tufvesson, and T. L. Marzetta, "Massive mimo for next generation wireless systems," *IEEE communications magazine*, vol. 52, no. 2, pp. 186–195, 2014.
- [2] X. Li, E. Leitinger, M. Oskarsson, K. Åström, and F. Tufvesson, "Massive mimo-based localization and mapping exploiting phase information of multipath components," *IEEE transactions on wireless communications*, vol. 18, no. 9, pp. 4254–4267, 2019.
- [3] A. Guerra, F. Guidi, and D. Dardari, "Position and orientation error bound for wideband massive antenna arrays," in *2015 IEEE International Conference on Communication Workshop (ICCW)*, pp. 853–858, IEEE, 2015.
- [4] H. Elsawy, W. Dai, M.-S. Alouini, and M. Z. Win, "Base station ordering for emergency call localization in ultra-dense cellular networks," *IEEE Access*, vol. 6, pp. 301–315, 2017.
- [5] A. Shahmansoori, G. E. Garcia, G. Destino, G. Seco-Granados, and H. Wymeersch, "Position and orientation estimation through millimeter-wave mimo in 5g systems," *IEEE Transactions on Wireless Communications*, vol. 17, no. 3, pp. 1822–1835, 2017.
- [6] A. Wang, L. Liu, and J. Zhang, "Low complexity direction of arrival (doa) estimation for 2d massive mimo systems," in *2012 IEEE Globecom Workshops*, pp. 703–707, IEEE, 2012.
- [7] D. Fan, F. Gao, Y. Liu, Y. Deng, G. Wang, Z. Zhong, and A. Nallanathan, "Angle domain channel estimation in hybrid millimeter wave massive mimo systems," *IEEE Transactions on Wireless Communications*, vol. 17, no. 12, pp. 8165–8179, 2018.
- [8] Z. Abu-Shaban, X. Zhou, T. Abhayapala, G. Seco-Granados, and H. Wymeersch, "Error bounds for uplink and downlink 3d localization in 5g millimeter wave systems," *IEEE Transactions on Wireless Communications*, vol. 17, no. 8, pp. 4939–4954, 2018.
- [9] E. Björnson, L. Sanguinetti, J. Hoydis, and M. Debbah, "Optimal design of energy-efficient multi-user mimo systems: Is massive mimo the answer?," *IEEE Transactions on Wireless Communications*, vol. 14, no. 6, pp. 3059–3075, 2015.
- [10] C. A. B. Camargo, G. Fraidenraich, and L. L. Mendes, "Probability of detection of the angle of arrival for massive mimo arrays," *IEEE Access*, vol. 6, pp. 65109–65117, 2018.
- [11] R. Miller and C. Chang, "A modified cramer-rao bound and its applications (corresp.)," *IEEE Transactions on Information theory*, vol. 24, no. 3, pp. 398–400, 1978.
- [12] A. N. D'Andrea, U. Mengali, and R. Reggiannini, "The modified cramer-rao bound and its application to synchronization problems," *IEEE Transactions on Communications*, vol. 42, no. 234, pp. 1391–1399, 1994.
- [13] K. Mahler, W. Keusgen, F. Tufvesson, T. Zemen, and G. Caire, "Tracking of wideband multipath components in a vehicular communication scenario," *IEEE Transactions on Vehicular Technology*, vol. 66, no. 1, pp. 15–25, 2016.
- [14] S. D. Bast and S. Pollin, "Mamimo csi-based positioning using cnns: Peeking inside the black box," *arXiv preprint arXiv:2003.04581*, 2020.
- [15] J. G. Andrews, S. Buzzi, W. Choi, S. V. Hanly, A. Lozano, A. C. Soong, and J. C. Zhang, "What will 5g be?," *IEEE Journal on selected areas in communications*, vol. 32, no. 6, pp. 1065–1082, 2014.
- [16] X. Gao, O. Edfors, F. Tufvesson, and E. G. Larsson, "Massive mimo in real propagation environments: Do all antennas contribute equally?," *IEEE Transactions on Communications*, vol. 63, no. 11, pp. 3917–3928, 2015.
- [17] M. Arash, E. Yazdian, M. S. Fazel, G. Brante, and M. A. Imran, "Employing antenna selection to improve energy efficiency in massive mimo systems," *Transactions on Emerging Telecommunications Technologies*, vol. 28, no. 12, p. e3212, 2017.
- [18] F. Reichenbach, J. Blumenthal, and D. Timmermann, "Comparing the efficiency of localization algorithms with the power-error-product (pep)," in *2008 The 28th International Conference on Distributed Computing Systems Workshops*, pp. 150–155, IEEE, 2008.
- [19] D. Lieckfeldt, J. You, J. Salzmann, R. Behnke, and D. Timmermann, "Characterizing the energy efficiency of localization algorithms in wireless sensor networks," in *Proceedings of the 2009 International Conference on Wireless Communications and Mobile Computing: Connecting the World Wirelessly*, pp. 839–843, ACM, 2009.

- [20] R. Couillet and M. Debbah, *Random matrix methods for wireless communications*. Cambridge University Press, 2011.
- [21] W. W.-L. Li, Y. Shen, Y. J. Zhang, and M. Z. Win, "Robust power allocation for energy-efficient location-aware networks," *IEEE/ACM Transactions on Networking*, vol. 21, no. 6, pp. 1918–1930, 2013.
- [22] H. Sallouha, A. Chiumento, S. Rajendran, and S. Pollin, "Localization in ultra narrow band iot networks: Design guidelines and tradeoffs," *IEEE Internet of Things Journal*, vol. 6, no. 6, pp. 9375–9385, 2019.
- [23] Y. Shen and M. Z. Win, "Fundamental limits of wideband localization—part i: A general framework," *IEEE Transactions on Information Theory*, vol. 56, no. 10, pp. 4956–4980, 2010.
- [24] A. C. Gurbuz and B. A. Cetiner, "Crlb based mode selection and enhanced doa estimation for multifunctional reconfigurable arrays," *Physical Communication*, vol. 38, p. 100894, 2020.
- [25] S. Wang and D. Byrne, "Angle of arrival detection system and method," May 24 2018. US Patent App. 15/357,976.
- [26] X. Zhang, L. Xu, L. Xu, and D. Xu, "Direction of departure (dod) and direction of arrival (doa) estimation in mimo radar with reduced-dimension music," *IEEE communications letters*, vol. 14, no. 12, pp. 1161–1163, 2010.
- [27] C. Stoeckle, J. Munir, A. Mezghani, and J. A. Nossek, "Doa estimation performance and computational complexity of subspace-and compressed sensing-based methods," in *WSA 2015; 19th International ITG Workshop on Smart Antennas*, pp. 1–6, VDE, 2015.
- [28] S. Boyd and L. Vandenberghe, *Convex optimization*. Cambridge university press, 2004.

APPENDIX A

PROOF OF THEOREM 1

Generally, \mathbf{X} is a complex matrix, composed from two real and imaginary parts, so we can write it as

$$\mathbf{X} = \Sigma^{\frac{1}{2}} (\mathbf{A} + j\mathbf{B})\mathbf{D}, \quad (53)$$

where

$$\Sigma = \beta^2 \sigma_h^2 \begin{bmatrix} 1 & 0 & \dots & 0 \\ 0 & 4 & & \vdots \\ \vdots & & \ddots & \\ 0 & \dots & & M^2 \end{bmatrix}, \quad (54)$$

and \mathbf{D} is a diagonal matrix with

$$D_{k,k} = \frac{|s_k|}{\sqrt{l(r_k)}}, \quad (55)$$

Choosing an arbitrary element of \mathbf{A} , we have

$$\begin{aligned} \mathbf{A}_{m,k} &= \frac{1}{\sqrt{M\sigma_h^2}} \operatorname{Re}\{h_{m,k} e^{-j(m\beta \cos(\theta_k) + \varphi_k)}\} \\ &= \frac{1}{\sqrt{M\sigma_h^2}} (h_{m,k}^r \cos(m\beta \cos(\theta_k) + \varphi_k) \\ &\quad + h_{m,k}^i \sin(m\beta \cos(\theta_k) + \varphi_k)), \end{aligned} \quad (56)$$

where φ_k is phase of k th transmitted pilot. So the variance of each element will be

$$\begin{aligned} \mathbb{E}\{\mathbf{A}_{m,k} \mathbf{A}_{m,k}^*\} &= \frac{1}{M\sigma_h^2} \mathbb{E}\{|h_{m,k}^r|^2\} \cos^2(m\sqrt{\beta} \cos(\theta_k) \\ &\quad + \varphi_k) + \frac{1}{M\sigma_h^2} \mathbb{E}\{|h_{m,k}^i|^2\} \sin^2(m\sqrt{\beta} \cos(\theta_k) + \varphi_k) = \frac{1}{M}. \end{aligned} \quad (57)$$

Similarly, $\mathbb{E}\{\mathbf{B}_{m,k} \mathbf{B}_{m,k}^*\} = \frac{1}{M}$. So, each element in \mathbf{A} and \mathbf{B} has same variance, equal to σ^2 , fourth and eighth moment of

order $\mathcal{O}(\frac{1}{M^2})$ and $\mathcal{O}(\frac{1}{M^4})$, respectively. If we replace Eq. 53 in $\mathbf{X}^H \mathbf{X}$, we have

$$\begin{aligned} \mathbf{X}^H \mathbf{X} &= \mathbf{D}(\mathbf{A} + j\mathbf{B})^H \boldsymbol{\Sigma} (\mathbf{A} + j\mathbf{B}) \mathbf{D} \\ &= \mathbf{D}(\mathbf{A}^T \boldsymbol{\Sigma} \mathbf{A} + \mathbf{B}^T \boldsymbol{\Sigma} \mathbf{B}) \mathbf{D} \\ &\quad + j\mathbf{D}(\mathbf{A}^T \boldsymbol{\Sigma} \mathbf{B} - \mathbf{B}^T \boldsymbol{\Sigma} \mathbf{A}) \mathbf{D}. \end{aligned} \quad (58)$$

Therefore

$$\mathcal{R}e(\mathbf{X}^H \mathbf{X}) = \mathbf{D}(\mathbf{A}^T \boldsymbol{\Sigma} \mathbf{A} + \mathbf{B}^T \boldsymbol{\Sigma} \mathbf{B}) \mathbf{D}. \quad (59)$$

Rewriting \mathbf{A} as

$$\mathbf{A} = [\mathbf{a}_1 \mathbf{a}_2 \dots \mathbf{a}_K]. \quad (60)$$

From Lemma 1 and Lemma 2 we have

$$\begin{aligned} \mathbf{a}_1^H \boldsymbol{\Sigma} \mathbf{a}_1 - \frac{1}{M} \text{tr}(\boldsymbol{\Sigma}) &\xrightarrow{a.s.} 0, \\ \mathbf{a}_2^H \boldsymbol{\Sigma} \mathbf{a}_2 - \frac{1}{M} \text{tr}(\boldsymbol{\Sigma}) &\xrightarrow{a.s.} 0, \\ \mathbf{a}_1^H \boldsymbol{\Sigma} \mathbf{a}_2 &\xrightarrow{a.s.} 0, \\ \mathbf{a}_2^H \boldsymbol{\Sigma} \mathbf{a}_1 &\xrightarrow{a.s.} 0. \end{aligned}$$

So, we can write

$$\begin{bmatrix} \mathbf{a}_1^H \\ \mathbf{a}_2^H \end{bmatrix} \boldsymbol{\Sigma} \begin{bmatrix} \mathbf{a}_1 & \mathbf{a}_2 \end{bmatrix} - \frac{1}{M} \begin{bmatrix} \text{tr}(\boldsymbol{\Sigma}) & 0 \\ 0 & \text{tr}(\boldsymbol{\Sigma}) \end{bmatrix} \xrightarrow{a.s.} \mathbf{0}_2. \quad (61)$$

After repeating this process for K columns of \mathbf{A} , we will have

$$\mathbf{A}^H \boldsymbol{\Sigma} \mathbf{A} - \frac{1}{M} \text{tr}(\boldsymbol{\Sigma}) \mathbf{I}_K \xrightarrow{a.s.} 0. \quad (62)$$

Similarly,

$$\mathbf{B}^H \boldsymbol{\Sigma} \mathbf{B} - \frac{1}{M} \text{tr}(\boldsymbol{\Sigma}) \mathbf{I}_K \xrightarrow{a.s.} 0. \quad (63)$$

Based on 62 and 63 and the fact that both \mathbf{A} and \mathbf{B} consist of real elements, we can write

$$\mathbf{A}^T \boldsymbol{\Sigma} \mathbf{A} + \mathbf{B}^T \boldsymbol{\Sigma} \mathbf{B} - \frac{2}{M} \text{tr}(\boldsymbol{\Sigma}) \mathbf{I}_K \xrightarrow{a.s.} 0. \quad (64)$$

Consequently

$$(\mathbf{A}^T \boldsymbol{\Sigma} \mathbf{A} + \mathbf{B}^T \boldsymbol{\Sigma} \mathbf{B})^{-1} - \frac{M}{2\text{tr}(\boldsymbol{\Sigma})} \mathbf{I}_K \xrightarrow{a.s.} 0. \quad (65)$$

Defining $\mathbf{C} \triangleq \sigma_n^2 \mathbf{D}^{-2}$ and noting that

$$\text{tr}(\boldsymbol{\Sigma}) = \beta^2 \sigma_h^2 \sum_{m=1}^M m^2 = \frac{\beta^2 \sigma_h^2 M(M+1)(2M+1)}{6}, \quad (66)$$

we obtain

$$\begin{aligned} \mathbf{CRLB}_{\cos(\theta)} &= \\ \frac{\sigma_n^2}{2} (\mathcal{R}e(\mathbf{X}^H \mathbf{X}))^{-1} &\xrightarrow{a.s.} \frac{3}{2\beta^2 \sigma_h^2 (M+1)(2M+1)} \mathbf{C}. \end{aligned} \quad (67)$$

□

APPENDIX B PROOF OF THEOREM 2

Defining \mathbf{E} as diagonal matrix with k th diagonal element as

$$\mathbf{E}_{k,k} \triangleq \sin^2(\theta_k), \quad (68)$$

when $\boldsymbol{\eta}_\theta$ has the form as in Eq. 23, Eq. 17 will be

$$\left(\frac{\partial \mathbf{w}}{\partial \boldsymbol{\eta}_\theta} \right) = -\mathbf{X} \mathbf{E}. \quad (69)$$

So

$$\begin{aligned} \mathbf{CRLB}_\theta &= \mathbf{J}_\theta^{-1} = (\mathcal{R}e([\left(\frac{\partial \mathbf{w}}{\partial \boldsymbol{\eta}} \right)^H \left(\frac{\partial \mathbf{w}}{\partial \boldsymbol{\eta}} \right)]])^{-1} \\ &= \frac{\sigma_n^2}{2} (\mathcal{R}e(\mathbf{E}^{\frac{1}{2}} \mathbf{X}^H \mathbf{X} \mathbf{E}^{\frac{1}{2}}))^{-1} \\ &\stackrel{a}{=} \frac{\sigma_n^2}{2} \mathbf{E}^{-\frac{1}{2}} (\mathcal{R}e(\mathbf{X}^H \mathbf{X}))^{-1} \mathbf{E}^{-\frac{1}{2}} \\ &\xrightarrow{a.s.} \frac{3}{2\beta^2 \sigma_h^2 (M+1)(2M+1)} \underbrace{\mathbf{E}^{-\frac{1}{2}} \mathbf{C} \mathbf{E}^{-\frac{1}{2}}}_{=\mathbf{S}}, \end{aligned} \quad (70)$$

Where $\stackrel{a}{=}$ follows from the fact that all elements of $\mathbf{E}^{\frac{1}{2}}$ are real. □